



HAL
open science

The role of the early diagenetic dolomitic concretions in the preservation of the 2.1-Ga paleoenvironmental signal: The Paleoproterozoic of the Franceville Basin, Gabon

Mavotchy Nathaelle Onanga, Abderrazak El Albani, Alain Trentesaux, Claude Fontaine, Anne-Catherine Pierson-Wickmann, Philippe Boulvais, Armelle Riboulleau, Lauriss Ngombi Pembed, Florent Pambo, François Gauthier-Lafaye

► To cite this version:

Mavotchy Nathaelle Onanga, Abderrazak El Albani, Alain Trentesaux, Claude Fontaine, Anne-Catherine Pierson-Wickmann, et al.. The role of the early diagenetic dolomitic concretions in the preservation of the 2.1-Ga paleoenvironmental signal: The Paleoproterozoic of the Franceville Basin, Gabon. *Comptes Rendus Géoscience*, 2016, 348 (8), pp.609-618. 10.1016/j.crte.2016.08.002 . insu-01390477

HAL Id: insu-01390477

<https://insu.hal.science/insu-01390477>

Submitted on 6 Jun 2017

HAL is a multi-disciplinary open access archive for the deposit and dissemination of scientific research documents, whether they are published or not. The documents may come from teaching and research institutions in France or abroad, or from public or private research centers.

L'archive ouverte pluridisciplinaire **HAL**, est destinée au dépôt et à la diffusion de documents scientifiques de niveau recherche, publiés ou non, émanant des établissements d'enseignement et de recherche français ou étrangers, des laboratoires publics ou privés.



ELSEVIER

Contents lists available at ScienceDirect

Comptes Rendus Geoscience

www.sciencedirect.com



Stratigraphy, Sedimentology (Palaeoenvironment)

The role of the early diagenetic dolomitic concretions in the preservation of the 2.1-Ga paleoenvironmental signal: The Paleoproterozoic of the Franceville Basin, Gabon



Nathaelle Onanga Mavotchy^a, Abderrazak El Albani^{a,*}, Alain Trentesaux^b, Claude Fontaine^a, Anne-Catherine Pierson-Wickmann^c, Philippe Boulvais^c, Armelle Riboulleau^b, Lauriss Ngombi Pemba^d, Florent Pambo^e, François Gauthier-Lafaye^f

^a Institut de chimie des milieux et matériaux de Poitiers (IC2MP), UMR 7285 CNRS–INSU–INC, université de Poitiers, 86000 Poitiers, France

^b Laboratoire d'océanologie et de géosciences (LOG), UMR 8187 CNRS, université de Lille, 59655 Villeneuve d'Ascq cedex, France

^c OSUR, laboratoire de géosciences, UMR 6118 CNRS, université de Rennes-1, 35000 Rennes, France

^d Université des sciences et techniques de Masuku, Franceville, Gabon

^e Société COMILOG, groupe ERAMET, Moanda, Gabon

^f Laboratoire d'hydrologie et de géochimie de Strasbourg, UMR 7517 CNRS, 67084 Strasbourg, France

ARTICLE INFO

Article history:

Received 26 May 2016

Accepted after revision 16 August 2016

Available online 27 October 2016

Handled by Sylvie Bourquin

Keywords:

Concretions

Paleoproterozoic

Francevillian

Palaeoenvironment

Gabon

ABSTRACT

Dolomite concretions from Paleoproterozoic organic-rich sediments of the Franceville Basin (Francevillian) in southeastern Gabon are studied. These concretions, belonging to one of the rare well-preserved Proterozoic sediments in the world, are mainly observed in the shaly levels of the Francevillian B1 Formation. The concretions often show a central pyrite-rich layer. The decrease in the carbonate content from the centre to the edges, and the carbon isotopic signal of carbonate within the concretions indicate a concentric growth of the concretions prior to compaction and precipitation of carbonate associated with the degradation of organic matter during early diagenesis. From its geochemical signature and texture, dolomite was not recrystallized. Moreover, the interior of the concretions shows well-preserved accumulations of microbial mats. These concretions thus appear to represent an exceptional record of the biogeochemical signature of the crucial period when the oxygen rose for the first time in Earth's atmosphere. If their rare-earth element pattern does not seem to reflect that of Paleoproterozoic seawater, they appear as potential tools for estimating the original oceanic temperature in surface sediments.

© 2016 Académie des sciences. Published by Elsevier Masson SAS. This is an open access article under the CC BY-NC-ND license (<http://creativecommons.org/licenses/by-nc-nd/4.0/>).

1. Introduction

Authigenic carbonate *s.l.* (calcite, dolomite) is produced in sediments during early diagenetic reactions, primarily associated with oxidation of organic matter through sulphate and iron reduction (i.e. Schrag et al., 2013), or by aerobic respiration (Coleman, 1985; Gautier and

* Corresponding author.

E-mail address: Abder.albani@univ-poitiers.fr (A. El Albani).

Claypool, 1984). Dolomite concretions are common in sedimentary rocks of all geological ages (Marshall and Pirrie, 2013), and are particularly present in organic-matter-rich sediments (Coleman, 1985; Curtis, 1977). Indeed, bacterial oxidation of organic matter locally increases the alkalinity of sediment pore water, thus favouring the growth of concretions (e.g., Bryce and Knauth, 1992; Gautier and Claypool, 1984; Hoareau et al., 2009; Hudson, 1978).

Carbonate concretions are developed in a variety of host rocks, including shales and sandstones. They display different shapes and sizes, ranging from septarian cracks in mudstones (Boles et al., 1985; Thyne and Boles, 1989), circular or ovoid shape (i.e. cannonball concretions; McBride et al., 2003), or sheet-like bodies (i.e. elongate concretions) in sediment rocks related to the influence of groundwater movement. Carbonate concretions are composed of calcite, dolomite, ankerite, siderite and rarely ferroan magnesite of varied chemical composition. Concretions can be produced by simple cementation in sediment pores (e.g., Curtis et al., 1986; Raiswell, 1971), by cementation in pores plus replacement of detrital grains, or by pushing the surrounding sediment (e.g., Chowns and Elkins, 1974) or rock, during early or late diagenesis.

Carbonate concretions usually show chemical changes from the core toward the edges (Curtis et al., 1986; Gautier, 1982; Irwin, 1980). These changes are explained in terms of progressive variations in pore-water composition, allowing tracing the diagenetic evolution of the pore-water chemistry (e.g., Mozley, 1996; Raiswell and Fisher,

2000). In particular, stable isotope data ($\delta^{13}\text{C}$ and $\delta^{18}\text{O}$) are used to address microbial activity in sediment porewater and ambient temperature of formation (McArthur et al., 1986; Ritger et al., 1987). Significant data on the biogeochemical cycle of carbon in the geological past have been provided by studies of carbon isotope variations in limestones and dolostones (e.g., Hotinski et al., 2004; Izon et al., 2015; Veizer and Hoefs, 1976). Nevertheless, similarly to oxygen, the carbon isotopic composition of carbonates is likely to change in response to re-crystallization during deep-burial diagenesis and low-grade metamorphism (e.g., Bryce and Knauth, 1992). Thus, the preservation of the pristine isotopic composition of Precambrian carbonates is often questioned (e.g., Veizer, 1989).

In the Francevillian basin (Fig. 1), dolomites are observed in the Francevillian B Formation (FB1; Fig. S1). They are mainly found in more or less organic matter-rich dolomitic black-shale horizons or as cement of sandstones deposits. The $\delta^{13}\text{C}$ values observed in these dolomites show a positive signal corresponding to the Lomagundi-Jatuli Event (Bekker et al., 2004; Melezhik et al., 2004), the origin of which is generally related with oxidative weathering of organic carbon-rich deposits under elevated levels of atmospheric oxygen (e.g., Bekker and Holland, 2012; Canfield et al., 2013; Holland, 2002). In the Moanda area, known for its manganiferous dolomite deposits, dolomitic concretions can be observed within silty black shales. They correspond to the unique example of dolomitic concretions observed in the Francevillian formations.

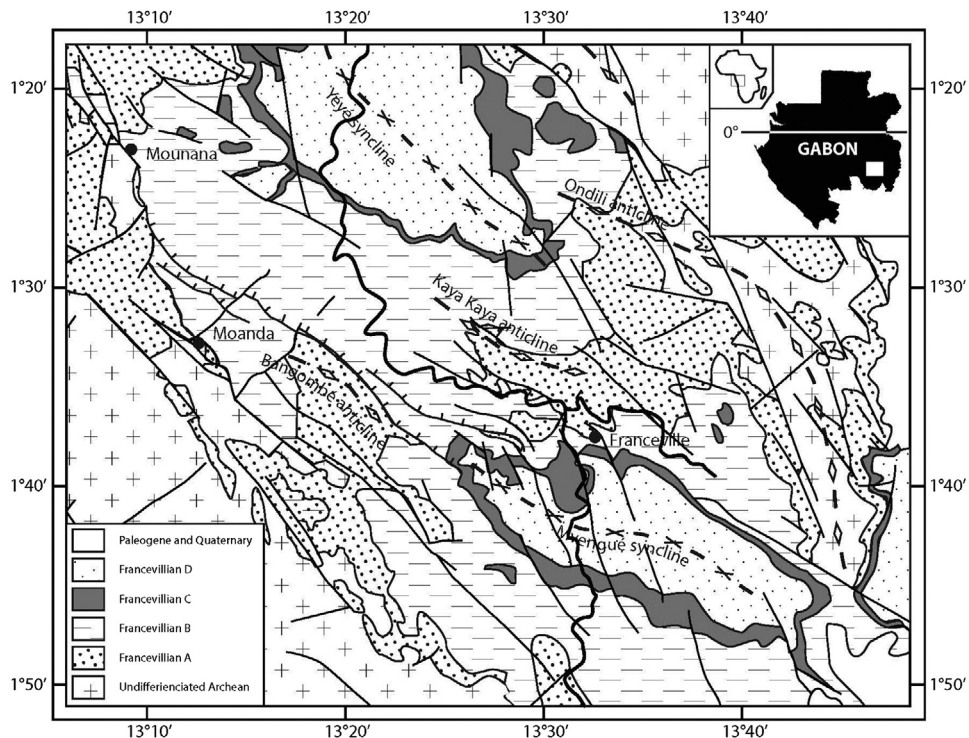


Fig. 1. Geological setting of Franceville Basin in Gabon (after Chevallier et al., 2002).

Here, we report a multi-approach study of selected dolomitic concretions from the Francevillian B1 Formation in Moanda area. The aims of this study are the understanding of the mechanism of concretionary growth. Furthermore, considering that concretions formed during the early diagenesis stage, the geochemical data are tested as proxies of environmental conditions during the first period of increased oxic conditions in the atmosphere.

2. Geological setting

2.1. The Francevillian Basin

The Francevillian Basin (Fig. 1) is a large foreland basin containing 35,000 km² of unmetamorphosed and undeformed sedimentary rocks. Strata were deposited in an epicontinental setting and crop out in the southeastern Republic of Gabon. The series, 1000 to 2500 m thick, are subdivided into four lithostratigraphic units, FA to FD

(Fig. S1), which rest unconformably on the Archean basement rocks (Weber, 1969; Pr at et al., 2011). The FA formation is essentially formed of fluvial and deltaic sandstone deposits; the FB formation consists of marine sediments and is further subdivided in several subunits; the previously reported large colonial organisms (El Albani et al., 2010, 2014), were collected from the FB2b black shales; the FC formation is dominated by dolomites and stromatolitic cherts; the FD formation corresponds to black shales. More detailed geological information is supplied as supplementary material.

2.2. Dolomitic concretions

The sedimentary sequence visible in the Moanda section is about 36 m in thickness (Fig. 2). It corresponds to the middle part of the FB1 Formation (about 2.1 Ga; Figs. 2, S1). It is characterised by an organic matter-rich clay-silt facies where centimetre-scale silt-sandstone

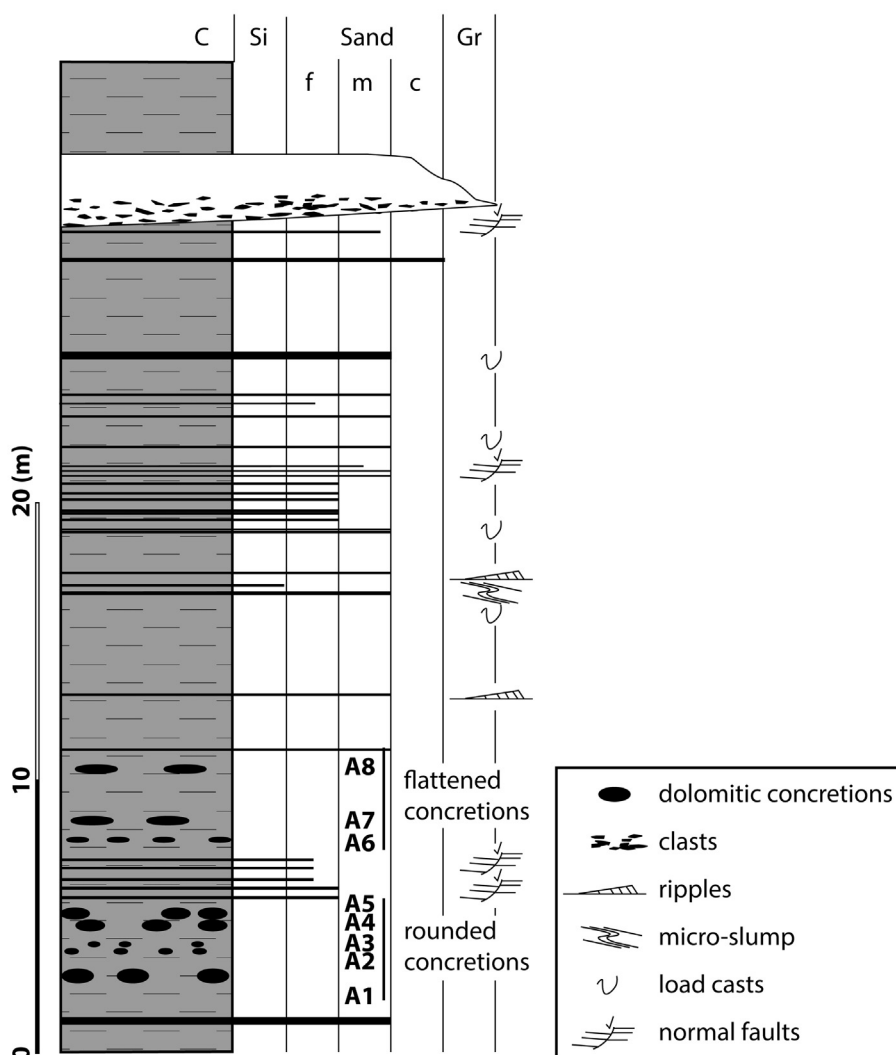


Fig. 2. Lithology of black shales sequence (FB1) at the Moanda area. Location of alignments of concretion samples.

horizons and carbonate concretions are intercalated. The uppermost part of the section is characterised by a microconglomeratic channel interval.

The sequence begins with black shales in which centimetre-scale silt–sandstone levels are intercalated as well as alignments of carbonate concretions, set parallel to the general stratification plane (Fig. 2). The black shales are finely horizontally laminated, which is typical of sedimentation in a quiet environment. The concretions are mainly observed in the lower 12 m of the section and are distributed within eight horizons (A1 to A8; Fig. S2). The concretions have various morphologies: rounded (Fig. S3A) to ellipsoidal (Fig. S3B), oblong, or flattened (Fig. S3C). Their lateral extension can reach 2 m, whereas their thickness rarely exceeds 40 cm. The most rounded concretions are located in the lowermost part of the section (Figs. S2A, S3). The concretions become lenticular, with a growing flattening degree toward the upper part of the section. No geometrical relationship suggesting a genetic link was observed between the position of the concretions and that of the silt–sandstone beds. In the upper half of the black shales,

the carbonate concretions disappear (Fig. S2B), whereas siliciclastic materials become more abundant, showing some load cast, centimetric slumping, and small synsedimentary faults characterising a high sedimentation rate. At the top of the sequence, a 2.4-m-thick microconglomeratic bed is deposited above the silty black shales. The base of this conglomeratic interval is erosive and affects the underlying silty black-shales, producing some synsedimentary normal faulting below the erosional surface.

To illustrate the internal structure of the concretions, we describe a section through an ovoid concretion found in alignment A5 (Fig. S2B). The 30-cm-thick concretion is divided into two roughly equal parts by a 3-mm-thick stripe of massive pyrite (Fig. 3A, B). Vertically, on each side of the pyrite stripe, dark laminations, which are more numerous in the lower part than in the upper part of the concretion, can be observed (Fig. S3A). Laterally, these sub-horizontal laminations bend towards the median part of the concretion (Fig. 3B, C), in a similar fashion to laminations in the enclosing black shale bend around the concretions (Fig. S3A, B, E, F).

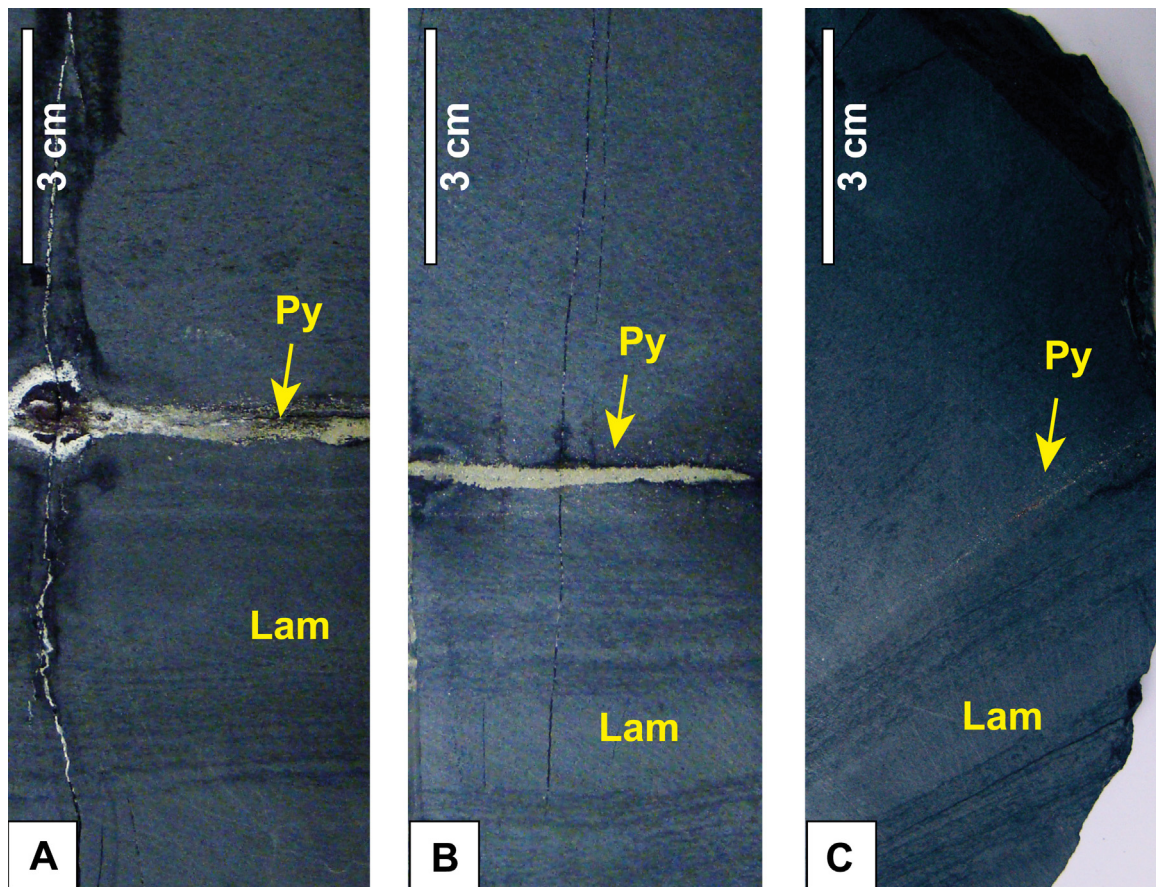


Fig. 3. Section through an ovoid concretion in alignment A5 showing its internal structure. (A) Pyrite stripe (Py), parallel to the stratification, divides the concretion into two equal parts. (B) Sub-planar laminations (Lam) on both sides of the pyrite stripe, clearer in the lower part of the concretion. (C) Laminations showing a flexure on the lateral edges of the concretion.

3. Results

3.1. Mineralogy

The centre of the concretion is filled with a millimetre-scale stripe of massive pyrite enclosed in a material composed of dolomite associated with small amounts of quartz and pyrite, traces of plagioclase feldspar, and clay minerals like chlorite and mica (Fig. S4A). Moving toward the upper, lower (Fig. S4B), and lateral edges (Fig. S4C) of the concretion, the quartz and clay minerals content increases. The transition to the black-shale host rock (Fig. S4D) is characterised by a marked drop in the dolomite content and a concomitant rise in quartz, plagioclase and all clay minerals, particularly with the occurrence of an interstratified illite/smectite mineral observed in this formation by Ngombi-Pemba et al. (2014) (see also Ossa Ossa et al., 2013).

Whereas the dolomite content is between 20 and 40% in the black shale, it can exceed 70% in the carbonate concretions. Detailed analysis of X-ray diffractions (XRD) of dolomite reflections indicates that two types of dolomite are present. One is pure dolomite, the other is ferroan dolomite. The abundance of ferroan dolomite increases towards the edges of the concretion (Suppl. Table 1).

3.2. Petrography

Texturally, the concretions are mainly composed of very fine dolomudstone facies. Pure dolomite is present in all parts of the concretions. Ferriferous dolomite is only observed at the external part of the nodules, where it appears as overgrowth on pure dolomite crystals (Fig. S5A).

In the lower half of the concretion, parallel and continuous black laminae rich in wavy organic matter (Fig. S5B) alternate with white dolomitic laminae. At the top of the concretion, laminae disappear and organic matter appears as patches scattered within the carbonate matrix (Fig. S5D). In the vicinity of the central pyrite stripe, a very homogeneous and structureless micritic matrix without organic matter can be observed (Fig. S5C). Organic matter patches without obvious orientation becomes visible again above the pyritous bed. Locally, part of the porosity near the host rocks is filled with pyrite, secondary recrystallization of quartz and alumino-silicate, more rarely by bundles of very fine calcite crystals typical of fast crystallization.

The central pyrite stripe is dominated by a compact aggregate of automorphic to sub-automorphic pyrite crystals with a mean size of 200 μm (Fig. S5F). Toward the lateral edges of the concretion, the pyritous stripe becomes discontinuous (Fig. S5C), showing aggregate morphologies. Toward the top and lower parts of the concretions, the pyrite grains are disseminated within the dolomitic matrix (Fig. S5E). Their size does not exceed 150 μm . Pyrite is automorphic to sub-automorphic. The pyrite grains are unaltered, indicating the good conservation of the system.

3.3. Geochemistry

Major, minor, trace and rare-earth element (REE) contents were analysed in detail in two concretions from alignment A5 and their immediately surrounding black shale. The results are highly comparable for the two concretions (Suppl. Table 2), and only one concretion (nodule N1) is detailed here.

3.4. Major elements

Across the transition between concretion and host rock, there is a drop in MgO and CaO contents and, conversely, an increase in SiO₂, Al₂O₃, Na₂O and K₂O contents (Suppl. Table 2), consistent with the mineralogical evolution observed from dolomite to a quartz, plagioclase and clay minerals assemblage. Total iron contents are lower in the host rock than in the concretion, which can be correlated with the occurrence of pyrite, mainly, and ferroan dolomite in the concretion. However, the iron content remains relatively constant ($4.45 \pm 0.35\%$) within the concretion, despite the variation in the proportion of pyrite and ferriferous dolomite. The presence of chlorite in the host rock prevents comparing the CaO/MgO ratio of dolomite in the black shale to that of dolomite in the concretion. MnO contents are three times higher in the concretion than in the rock host.

3.5. Trace and rare-earth elements

Most trace elements are depleted in the concretion compared to the values observed in the black shale (Fig. 4A, Suppl. Tab. 2). The depletion coefficients vary from 50 to 80% (mean of 67%). Conversely, the concentration of strontium increases in the concretion, in parallel to the concentration of carbonate (Fig. 4A; Suppl. Tab. 2). Fig. 4B illustrates the negative correlation with strontium observed for most elements: elements associated to the detrital phase (e.g., Rb), elements generally associated with organic matter (e.g., Ba), and redox-sensitive elements (e.g., V). This negative correlation clearly points to sediment dilution by carbonates within the nodule.

When element concentrations are normalised to the aluminium content, two behaviours are observed (not shown): 1) a more or less constant element/Al ratio in the concretion and in the black shale (e.g., Ti, Rb, Zr, Th, Cr); 2) a decrease of the element/Al ratio from the concretion to its border and the enclosing black shale (e.g., Sr, Ba, Co, Ni, Zn, U, Pb, V). The first group corresponds to elements considered as conservative and generally associated with the detrital phase. The second group corresponds to elements often incorporated in authigenic minerals: Sr in carbonates, Ba, Co, Ni, U, V, Zn, and Pb, in minerals precipitated in association with organic matter diagenesis, particularly in reducing environments (Tribouillard et al., 2006). The Ba/Al, Co/Al, Ni/Al, U/Al, and Zn/Al ratios of the black shale are similar to the Post Archean Australian Shale (PAAS) values (Taylor and McLennan, 1985).

Like all metals, the content of rare-earth elements decays from the black shale to the centre of the concretion (Suppl. Tab. 2). After normalization to the PAAS standard

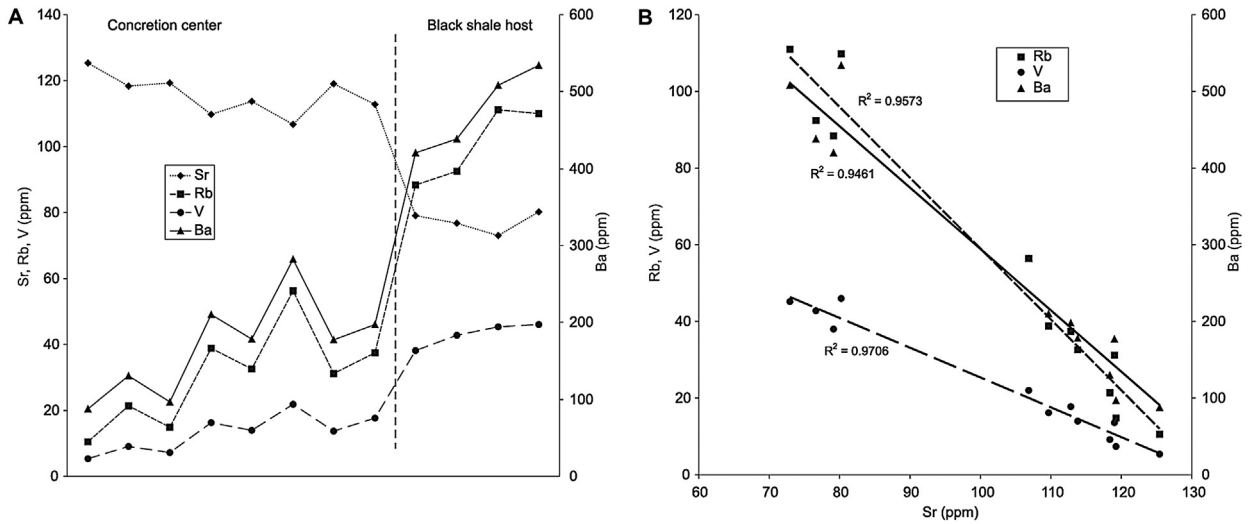


Fig. 4. Concentration of selected trace elements in the concretion of alignment A5. (A) Evolution of the rubidium (Rb), strontium (Sr), vanadium (V), and barium (Ba) concentrations from the concretion's centre to the black shale. (B) Inverse correlation of rubidium, vanadium and barium contents with strontium concentration.

(Taylor and McLennan, 1985), the black-shale host rock (Fig. S6) shows a light rare-earth-element-enriched pattern ($(La/Lu)_{SN} = 1.8$ to 3.0). This signature is absent at the centre of the nodule, where $(La/Lu)_{SN} = 1$, but is visible at the edge of the concretion, with $(La/Lu)_{SN}$ ranging up to 2.8 (Suppl. Table 2).

3.6. C and O isotopes

The $\delta^{18}O$ values (PDB) of the black shales range between -11.1 and -9.6% , with a mean of $-10.4 \pm 0.6\%$, while those of the concretions are between -9.8 and -6.3% (Fig. 5, Suppl. Tab. 2). The $\delta^{13}C$ values (PDB)

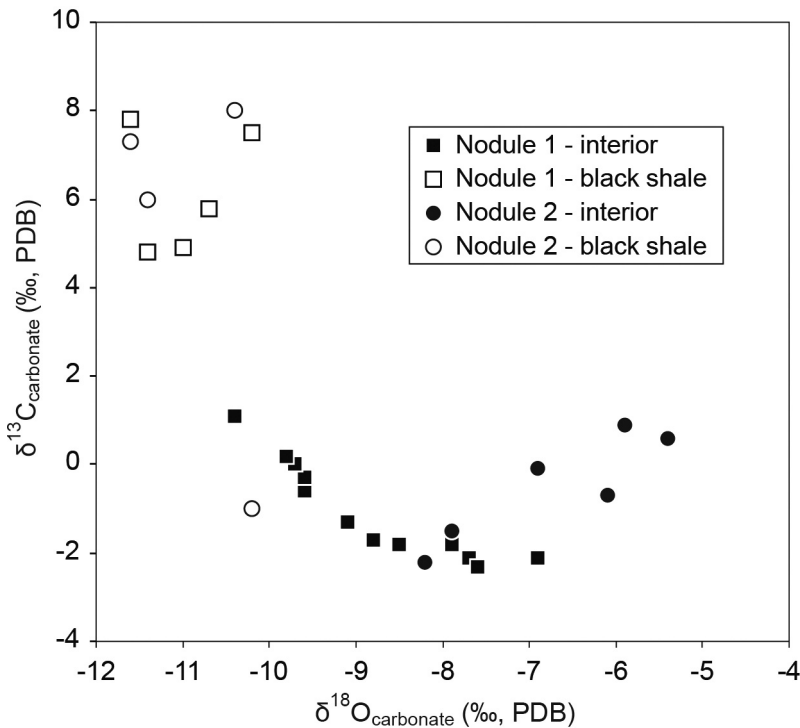


Fig. 5. Cross plot of carbon and oxygen isotope composition of the two dolomitic concretions from alignment A5 and the black-shale host rock.

of the dolomites from the black shales are between -1.0 and $+7.8\%$, with a mean of $+5.7 \pm 2.8\%$, while those of the concretions range between -2.3 and $+1.1$. For the organic fraction of the black shales, the $\delta^{13}\text{C}_{\text{org}}$ values (PDB) range between -29.4 and -24.9% , with a mean of $-25.5 \pm 1.5\%$, while those of the concretions range between -26.5 and -25.1% , with a mean of $-25.9 \pm 0.5\%$.

Within one of the two concretions, radial (centre-to-edge) variations in both $\delta^{13}\text{C}$ and $\delta^{18}\text{O}$ values are visible (Fig. S7). In nodule N1, the $\delta^{13}\text{C}$ values tend to increase toward the edges, getting closer to the values observed in black shale host rocks (Fig. S7C, Suppl. Tab. 2). The $\delta^{18}\text{O}$ values show a slight decrease from the centre to the borders (Fig. S7D). In nodule N2, the isotopic compositions of the carbonate fraction are more erratic; nevertheless, similarly to nodule N1, the carbon isotopic values are lower, while oxygen isotopic values are higher than in the black shale (Fig. 5).

4. Discussion

4.1. Depositional setting

In argillaceous sediments, compaction generally controls the morphology of concretions (El Albani et al., 2001, 2002; Hudson, 1978; Marshall and Pirrie, 2013). Freshly deposited sediment contains a high proportion of interstitial water, up to 80%, which is gradually forced out during burial under the increasing lithostatic pressure (Marshall and Pirrie, 2013). As a consequence of compaction, sediment permeability becomes increasingly anisotropic, getting very low in the upward direction. Interstitial water thus migrates horizontally rather than vertically, which contributes to the growth of elongated concretions following the stratification plane of the host material (Hoareau et al., 2009). The rounded morphology of the basal carbonate concretions (alignments A1 to A5) in the Francevillian FB1 Formation indicates that they were formed in uncompacted sediments or sediments at the very beginning of their compaction. The concretions therefore likely formed during periods of low sedimentation rate, during early diagenesis (Canfield & Raiswell, 1991; Mozley, 1996; Raiswell, 1971, 1976, 1988).

The growth of more flattened concretions (alignments A6 to A8) indicates that the sedimentation rate gradually increased, accelerating compaction speed. The internal structure of lenticular concretions shows very well-preserved horizontal laminae, which were little affected by compaction before lithification. Nevertheless, the morphology of the contacts between the concretions and their host rocks (Figs. S3E, F) indicates that the formation occurred in an unconsolidated state (Canfield and Raiswell, 1991; Lash and Blood, 2004; Mozley, 1996).

The upwards disappearance of nodules is followed by an increase in the abundance of silt-sandstone beds showing ripples and loadcasts (Fig. 2). These features are indicative of a higher energy level, likely associated to a higher sedimentation rate. Early diagenetic cementation therefore stopped when the sedimentation rate increased.

4.2. Concretioning mechanisms

The studied concretions show a very similar internal structure organised around a pyrite stripe that seems to be their original nucleus. This nucleus likely corresponded to a bacterial microbial accumulation. Nevertheless, as indicated by the geochemical data (Suppl. Tab. 2) and by their structure at their periphery (Figs. 3C, S3), the concretions grew concentrically. The stable element/Al ratios for detrital elements in the concretions and black shales indicate that these concretions developed by cement precipitation in “free” pore spaces of the black-shale host rock (Raiswell, 1976). Considering that the remaining porosity is low (Raiswell and Fisher, 2000), the initial porosity can be estimated by converting the carbonate weight percentage in the concretion into the volume percentage of the initial void (Gautier, 1982). Using XRD analysis, the carbonate (dolomite) content obtained from different concretions ranges from 45 to 88% (mean of 64%). The amount decreases from the centre to the edges. This clearly indicates that the growth of concretions continued during burial by addition of successive cement layers (Mozley, 1996; Oertel and Curtis, 1972; Raiswell, 1971). Laminae in the host black shale are deformed around the concretions due to differential compaction (Lash and Blood, 2004; Oertel and Curtis, 1972).

Both the C isotope composition of the carbonate fractions (Figs. 5, S7, Suppl. Table 2) and the occurrence of the pyrite nucleus are consistent with an authigenic dolomitisation process related to the degradation of locally concentrated organic matter by bacterial sulphate reduction (Berner, 1980; Lash and Blood, 2004). Sulphate reduction increases alkalinity (Hardie, 1987) and favours dolomite precipitation as it removes dissolved sulphate, which inhibits dolomite precipitation (e.g., Baker and Kastner, 1981; Compton, 1988). The local abundance of organic matter in the sediment at the origin of nodule precipitation is suggested by the high Ba/Al ratio in the central part of the concretion, as barium is generally associated with organic matter (Tribouillard et al., 2006). The redox-sensitive trace elements ratios in the black shale, close to PAAS values, suggest that early diagenetic conditions in the hosting sediment were overall poorly reducing. Nevertheless, the higher element/Al ratios in the central part of the concretions indicate that reducing conditions locally developed in the sediment, in association with the degradation of the local concentrations of organic matter.

Oxidation of organic matter is generally considered as the main source of the carbonate ion (CO_3^{2-}) at the origin of carbonate concretions (Claypool and Kaplan, 1974; Irwin, 1980; Raiswell and Fisher, 2000). Bacterial oxidation of organic matter and sulphate reduction both produce ^{12}C -enriched CO_2 , while thermal decarboxylation and bacterial fermentation (methanogenesis) produce ^{12}C -depleted CO_2 (Claypool and Kaplan, 1974). The $\delta^{13}\text{C}$ of carbonate concretions thus depends on the source of carbonate ions present in pore waters. Carbonates deposited during the Lomagundi event are generally characterised by high $\delta^{13}\text{C}$ values (up to $+10\%$; Bekker and Holland, 2012), suggesting that carbonate dissolved in

seawater was enriched in ^{13}C compared to the current situation. Consistently, organic-poor shales and dolostones of the FB1 formation show an average $\delta^{13}\text{C}$ value around 5.4‰ (Ngombi-Pemba, 2014). The negative $\delta^{13}\text{C}$ encountered in Moanda carbonate concretions (with $\delta^{13}\text{C}$ down to -2.2 ‰ in the centre of the concretion) are consistent with a contribution of dissolved carbonate produced by bacterial sulphate reduction. On the other hand, the very positive $\delta^{13}\text{C}$ carbonate values in Moanda black shales ($\delta^{13}\text{C} \sim +7.8$ ‰) compared to organic-poor shales of the same age may result from bacterial fermentation.

The continuous precipitation of dolomitic concretions after the beginning of sediment compaction suggests that alkalinity and Ca and Mg contents remained at saturation values, allowing carbonate crystallization. Several authors (Lash and Blood, 2004; Raiswell, 1988) proposed anaerobic oxidation of biogenic methane (AOM) as a probable source of carbon for continued precipitation of carbonate concretions. Indeed, the biogenic methane produced by microbial decomposition of organic matter in the methanogenesis zone diffuses up to the base of the zone of sulphate reduction, where it is oxidized to CO_2 , allowing carbonate precipitation (Claypool and Kaplan, 1974). The dissolved CO_2 produced by AOM is isotopically light and may be poorly discernible from that produced by bacterial sulphate reduction of organic matter (Raiswell and Fisher, 2000). Below the zone of AOM, carbonate precipitation may be associated with the CO_2 liberated during bacterial methanogenesis, in which case precipitated carbonates will have a heavy isotopic signature (Lash and Blood, 2004).

From their mineral associations, Moanda concretions probably show a dolomitization phenomenon first controlled by bacterial sulphate reduction (pure dolomite + massive pyrite) then by the anaerobic oxidation of methane and finally methanogenesis (ferroan dolomite + rare pyrite). The increase of the Fe/Mn ratio from the centre (Fe/Mn ~ 12) towards the concretion edges (Fe/Mn > 26) is consistent with this scenario: Mn^{2+} ions are more stable in oxidizing conditions than Fe^{2+} while in presence of dissolved sulphides, Fe^{2+} rapidly forms pyrite. The outward increase in the Fe/Mn ratio is therefore consistent with progressive formation of the concretion in an increasingly reducing sediment (Boles et al., 1985) and precipitation of the outer margins of the concretion in a diagenetic zone where sulphide concentration is low, e.g., close to the zone of methanogenesis.

4.3. Recordings of paleoenvironmental variations

The rare-earth-element and yttrium (REE + Y) signatures of limestones and carbonate concretions are sometimes used as recorders of ancient seawater signatures (e.g., Nothdurft et al., 2004). The REE + Y pattern of Moanda concretions can therefore be evaluated. In general, terrigenous sediments contain relatively high REE + Y concentrations with non-seawater-like REE + Y patterns (Nothdurft et al., 2004). The host rock displays such PAAS-normalized REE + Y patterns (Fig. S6A). PAAS-normalized seawater-like REE + Y patterns generally exhibit the following features (Fig. S6B): (1) significant light REE

depletion, (2) negative Ce anomaly, though not always recorded in ancient rocks (Bau and Dulski, 1996), (3) slight positive La anomaly (e.g., Bau and Dulski, 1996; De Baar et al., 1991) and (4) superchondritic Y/Ho ratios (e.g., Bau, 1996). Such patterns are not observed in Moanda dolomitic concretions (Fig. S6A). The centre of the concretion whose signature is the most likely to reflect the composition of the earliest cementing fluid nevertheless contains a significant fraction of non-carbonate minerals. By making the simple assumption that the non-carbonate fraction corresponds to detrital minerals, the REE content of the carbonate phase ($\text{REE}_{\text{carbonate}}$) can be calculated as follows: $\text{REE}_{\text{carbonate}} = \text{REE-Al} \times (\text{REE/Al})_{\text{black shales}}$, where REE and Al are the elemental concentrations of the considered sample and $(\text{REE/Al})_{\text{black shales}}$ is the average REE/Al ratio in the host black shale. The $(\text{REE} + \text{Y})_{\text{carbonate}}$ patterns thus obtained using the two innermost samples in Moanda concretion N1 appear more “seawater-like” than the total sample, with a slight light REE depletion compared to HREE and a significant Y/Ho ratio (Fig. S6B). Nevertheless, as shown in Fig. S6B, the obtained pattern remains markedly different from that of present-day seawater and of Paleoproterozoic seawater, as documented in iron formations of the Transvaal Supergroup, South Africa (Bau and Dulski, 1996). This suggests that the REE + Y composition of porewater was rapidly influenced by redox conditions, but also likely by fluxes of dissolved REE from the underlying sediment (e.g., Elderfield and Sholkovitz, 1987).

The Moanda concretions apparently preserved the depositional fabric of the original sediments (Mozley, 1996). Good preservation suggests that carbonate cementation began early, close to the sediment/water interface (Raiswell, 1971, 1988), or during early diagenesis, before any significant compaction (Calvert et al., 1985; Canfield & Raiswell, 1991; Curtis et al., 1986; Mozley, 1996; Pruyssers et al., 1991). Nevertheless, we cannot rule out the overprint of later diagenesis. Based on the presence of mixed layer illite-smectite clay minerals (Ngombi-Pemba et al., 2014; Ossa Ossa et al., 2013), it is however suggested that the sediments of the FB Formation have been buried at a depth < 2000 m (Aoyagi and Kazama, 1980; Chamley, 1989; Chamley et al., 1990; Velde, 1995). The two studied nodules share identical isotopic compositions in their central part, and therefore appear as the most primitive values recorded in the system ($\delta^{18}\text{O}$ close to -7 ‰, $\delta^{13}\text{C}$ close to -2 ‰; Fig. 5). The oxygen isotope composition of early diagenetic dolomites forming in organic-rich sediments is relatively well understood: such dolomites begin to form a few centimetres below the sediment-water interface, where pore waters have $\delta^{18}\text{O}$ values similar to those of seawater (e.g., Kelts and McKenzie, 1982; Pisciotto and Mahoney, 1981). The oxygen isotope composition of the concretion is therefore mainly determined by the temperature of precipitation at a given $\delta^{18}\text{O}$ value of the water. Using several fractionation factors between dolomite and water available in the literature (Fritz and Smith, 1970; Matthews and Katz, 1977; Vasconcelos et al., 2005; Zheng, 1999) and using the $\delta^{18}\text{O}$ value for seawater of -8.5 ‰ (SMOW) at 2.1 Ga modelled by Jaffrés et al. (2007), the $\delta^{18}\text{O}$ value of -7 ‰ recorded in the centre of the nodules may thus be the sign of a temperature precipitation around

23 to 28 °C (Suppl. Table 3). Slightly higher precipitation temperatures (36 to 42 °C) are obtained using the alternative $\delta^{18}\text{O}$ value for seawater at 2.1 Ga of -6% (SMOW; Jaffrés et al., 2007, Suppl. Table 3). It is beyond the scope of this study to go further in the debates about the oxygen isotopic composition and temperature of seawater in the Paleoproterozoic, but it is worthy to mention that the temperatures calculated here are very similar to those of present-day shallow seawater.

5. Conclusion

The Paleoproterozoic organic-rich sediments of the Franceville Basin in southeastern Gabon contain dolomite concretions of various shapes and sizes. The internal structure of the concretions, the mineralogical assemblages and the geochemical signatures allow us to determine that these concretions: 1) are very well preserved; 2) began to form very early in the diagenesis process in relation to the degradation of local accumulations of organic matter by sulphate reduction; 3) grew concentrically during burial under the progressive influence of anaerobic oxidation of methane and then methanogenesis. Because of their very good preservation and their formation during early diagenesis, these dolomitic concretions may have preserved some information relative to the Paleoproterozoic paleoenvironmental conditions. If the REE pattern in the centre of the concretions appears not to record the REE pattern of seawater, their oxygen isotope composition might be a faithful recorder of seawater temperature. Provided that the estimates of Paleoproterozoic seawater $\delta^{18}\text{O}$ currently available are correct, the $\delta^{18}\text{O}$ value of $\sim -7\%$ recorded in the centre of the nodules indicates a precipitation temperature around 20–40 °C; these temperatures are very similar to those of present-day shallow seawater.

Acknowledgements

The authors wish to acknowledge the two reviewers, A. Loi and N. Tribouillard for constructive and helpful comments. The CNRS–INSU, FEDER, the University of Poitiers, the Région Poitou-Charente for financial support. The Gabon Ministry of Education and Research, CENAREST, the Gabon Ministry of Mines, Oil, Energy and Hydraulic Resources, the General Direction of Mines and Geology, as well as Sylvia Bongo (Ondimba Foundation), the 'Agence nationale des parcs nationaux' (Gabon), COMILOG, SOCOBA & Air-France Companies; the French Embassy at Libreville for collaboration and technical support. We are thankful to C. Laforest, A. Meunier, P. Recourt, J.-L. Albert, and N. Dauger for assistance.

Appendix A. Supplementary data

Supplementary data associated with this article can be found, in the online version, at <http://dx.doi.org/10.1016/j.crte.2016.08.002>.

References

- Aoyagi, K., Kazama, T., 1980. Transformational changes of clay minerals, zeolites and silica minerals during diagenesis. *Sedimentology* 27, 179–188.
- Baker, P.A., Kastner, M., 1981. Constraints on the formation of sedimentary dolomite. *Science* 213, 214–216.
- Bau, M., 1996. Controls on fractionation of isovalent trace elements in magmatic and aqueous systems: evidence from Y/Ho, Zr/Hf and lanthanide tetrad effect. *Contr. Mineral. Petrol.* 123, 323–333.
- Bau, M., Dulski, P., 1996. Distribution of yttrium and rare-earth elements in the Penge and Kuruman iron-formations, Transvaal Supergroup, South Africa. *Precamb. Res.* 79, 37–55.
- Bekker, A., Holland, H.D., Wang, P.L., Rumble III, D., Stein, H.J., Hannah, J.L., Coetzee, L.L., Beukes, N.J., 2004. Dating the rise of atmospheric oxygen. *Nature* 427, 117–120.
- Bekker, A., Holland, H.D., 2012. Oxygen overshoot and recovery during the Early Paleoproterozoic. *Earth Planet. Sci. Lett.* 317–318, 295–304.
- Berner, R.A., 1980. *Principles of Chemical Sedimentology*. McGraw-Hill (1971), New York, 240 p.
- Boles, J.R., Landis, C.A., Dale, P., 1985. The Moeraki Boulders; anatomy of some septarian concretions. *J. Sedim. Petrol.* 55 (3), 398–406.
- Bryce, W., Knauth, L.P., 1992. Stable isotope geochemistry of cherts and carbonates from the 2.0 Ga Gunflint Iron Formation: implications for the depositional setting and the effects of diagenesis and metamorphism. *Precamb. Res.* 59, 283–313.
- Calvert, S.E., Mokerjee, S., Morris, R.J., 1985. Trace metals in fulvic and humic acids from modern organic-rich sediments. *Oceanol. Acta* 8, 167–173.
- Canfield, D.E., Ngombi-Pemba, L., Hammarund, E.U., Bengtson, S., Chausson, M., Gauthier-Lafaye, F., Meunier, A., Riboulleau, A., Rollion-Bard, C., Rouxel, O., Asael, D., Pierson-Wickmann, A.-C., El Albani, A., 2013. Oxygen dynamics in the aftermath of the Great Oxidation of Earth's atmosphere. *PNAS* 110, 16736–16741.
- Canfield, D.E., Raiswell, R., 1991. Pyrite Formation and Fossil Preservation. In: Allison, P.A., Briggs, D.E.G. (Eds.), *Taphonomy: Releasing the Data Locked in the Fossil Record*. Plenum, New York, pp. 337–387.
- Chamley, H., 1989. *Clay sedimentology*. Springer-Verlag, Berlin, 623 p.
- Chamley, H., Deconinck, J.F., Millot, G., 1990. Sur l'abondance des minéraux smectitiques dans les sédiments marins communs déposés lors des périodes de haut niveau marin du Jurassique au Paléogène. *C. R. Acad. Sci. Paris Ser. II* 311, 1529–1536.
- Chevallier, L., Makanga, J.F., Thomas, R.J., 2002. Carte géologique de la République gabonaise, 1:1 000 000. Notice explicative. Council for Geoscience, South Africa, 195 p.
- Chowans, T.M., Elkins, J.E., 1974. The origin of quartz geodes and cauliflower chert through the silicification of anhydrite nodules. *J. Sedim. Petrol.* 44, 885–903.
- Claypool, G.E., Kaplan, I.R., 1974. The origin and distribution of methane in marine sediments. In: Kaplan, I.R. (Ed.), *Natural Gases in Marine Sediments*. Plenum Press, London, pp. 99–139.
- Coleman, M.L., 1985. Geochemistry of diagenetic nonsilicate minerals: kinetic considerations. *Phil. Trans. R. Soc. Lond. A* 315, 39–56.
- Compton, J.S., 1988. Degree of supersaturation and precipitation of organogenic dolomite. *Geology* 16, 318–321.
- Curtis, C.D., 1977. Sedimentary geochemistry: environments and processes dominated by involvement of an aqueous phase. *Phil. Trans. R. Soc. Lond. A* 268, 353–372.
- Curtis, C.D., Coleman, M.L., Love, L.G., 1986. Pore water evolution during sediment burial from isotopic and mineral chemistry of calcite, dolomite and siderite concretions. *Geochim. Cosmochim. Acta* 50, 2321–2334.
- De Baar, H.J.W., Schijf, J., Byrne, R.H., 1991. Solution chemistry of the rare earth elements in seawater. *Eur. J. Solid State Inorg. Chem.* 28, 357–373.
- El Albani, A., Vachard, D., Kuhnt, W., Thurow, J., 2001. The role of diagenetic carbonate concretions in the preservation of the original sedimentary record. *Sedimentology* 48, 875–886.
- El Albani, A., Cloutier, R., Candilier, A.M., 2002. Early diagenesis of the Upper Devonian Escuminac Formation in the Gaspé Peninsula, Quebec: sedimentological and geochemical evidence. *Sediment. Geol.* 146, 209–223.
- El Albani, A., Bengton, S., Canfield, D.E., Bekker, A., Miacchiarelli, R., Mazurier, A., Hammarlund, E.U., Boulvais, P., Dupuy, J.J., Fontaine, C., Füssi, F.T., Gauthier-Lafaye, F., Janvier, P., Javaux, E., Ossa-Ossa, F., Pierson-Wickmann, A.C., Riboulleau, A., Sardini, P., Vachard, D., Whitehouse, M., Meunier, A., 2010. Large colonial organisms with coordinated growth in oxygenated environments 2.1 billion years ago. *Nature* 466, 100–104.

- El Albani, A., Bengston, S., Canfeld, D., Riboulleau, A., Rollion-Bard, C., Macchiarelli, R., Ngombi-Pemba, L., Hammarlund, E., Meunier, A., Moule, I.M., Benzerara, K., Bernard, S., Boulvais, P., Chaussidon, M., Cesari, C., Fontaine, C., Chi-Fru, E., Ruiz, J.M.G., Gauthier-Lafaye, F., Mazurier, A., Pierson-Wickmann, A.-C., Rouxel, O., Trentesaux, A., Vecoli, M., Versteegh, G.J.M., White, L., Whitehouse, M., Bekker, A., 2014. The 2.1 Ga Old Francevillian Biota: Biogenicity, Taphonomy and Biodiversity. *Plos One* 9, e99438.
- Elderfield, H., Sholkovitz, E.R., 1987. Rare earth elements in the pore waters of reducing nearshore sediments. *Earth Planet. Sci. Lett.* 82 (3–4), 280–288.
- Fritz, P., Smith, D.G.W., 1970. The isotopic composition of secondary dolomite. *Geochim. Cosmochim. Acta* 34, 1161–1173.
- Gautier, D.L., 1982. Siderite concretions: indicators of early diagenesis in the Gammon shale (Cretaceous). *J. Sedim. Petrol.* 52, 859–871.
- Gautier, D.L., Claypool, G.E., 1984. Interpretation of methanic diagenesis in ancient sediments by analogy with processes in modern diagenetic environments. In: McDonald, D.A., Surdam, R.C. (Eds.), *Clastic Diagenesis*, 37, Mem. Am. Assoc. Petrol. Geol., pp. 111–123.
- Hardie, L.A., 1987. Perspective on dolomitization: a critical view of some current views. *J. Sedim. Petrol.* 57, 166–183.
- Hoareau, G., Odonne, F., Debroas, E.J., Maillard, A., Monnin, C., Callot, P., 2009. Dolomitic concretions in the Eocene Sobrarbe delta (Spanish Pyrenees): fluid circulation above a submarine slide scar infilling. *Mar. Petrol. Geol.* 26, 724–737.
- Holland, H.D., 2002. Volcanic gases, black smokers, and the great oxidation event. *Geochim. Cosmochim. Acta* 66, 3811–3826.
- Hotinski, R.M., Kump, L.R., Arthur, M.A., 2004. The effectiveness of the Paleoproterozoic biological pump: A $\delta^{13}\text{C}$ gradient from platform carbonates of the Pethe Group (Great Slave Lake Supergroup, NWT). *Geol. Soc. Am. Bull.* 116, 539–554.
- Hudson, J.D., 1978. Concretions, isotopes, and diagenetic history of Oxford Clay (Jurassic) of central England. *Sedimentology* 25, 339–369.
- Irwin, H., 1980. Early diagenetic carbonate precipitation and pore fluid migration in the Kimmeridge of Dorset, England. *Sedimentology* 27, 577–591.
- Izon, G., Zerkle, A.L., Zhelezinskaya, I., Farquhar, J., Newton, R.J., Poulton, S.W., Eigenbrode, J.L., Claire, M.W., 2015. Multiple oscillations in Neoproterozoic atmospheric chemistry. *Earth Planet. Sci. Lett.* 431, 264–273.
- Jaffrés, J.B.D., Shields, G.A., Wallmann, K., 2007. The oxygen isotope evolution of seawater: a critical review of a long-standing controversy and an improved geological water cycle model for the past 3.4 billion years. *Earth Sci. Rev.* 83, 83–122.
- Kelts, K.R., McKenzie, J.A., 1982. Diagenetic dolomite formation in Quaternary anoxic diatomaceous muds of Deep Sea Drilling Project, Leg 64, Gulf of California, 64, Initial Reports of the Deep Sea Drilling Project, pp. 553–569.
- Lash, G.G., Blood, D., 2004. Geochemical and textural evidence for early (shallow) diagenetic growth of stratigraphically confined carbonate concretions, Upper Devonian Rhinestreet black shale, western New York. *Chem. Geol.* 206, 407–424.
- Marshall, J.D., Pirrie, D., 2013. Carbonate concretions - explained. *Geol. Today* 29, 53–62.
- Matthews, A., Katz, A., 1977. Oxygen isotope fractionation during the dolomitization of calcium carbonate. *Geochim. Cosmochim. Acta* 41, 1431–1438.
- McArthur, J.M., Benmore, R.A., Coleman, M.L., Soldi, C., Yeh, H.W., O'Brien, G.W., 1986. Stable isotopic characterization of francolite formation. *Earth Planet. Sci. Lett.* 77, 20–34.
- McBride, E.F., Picard, M.D., Milliken, K.L., 2003. Calcite-Cemented Concretions in Cretaceous Sandstone, Wyoming and Utah, U.S.A. *J. Sedim. Res.* 73 (3), 462–483.
- Melezhik, V.A., Fallick, A.E., Grillo, S.M., 2004. Subaerial exposure features in a Palaeoproterozoic ^{13}C -rich dolostone sequence from the Pechenga Greenstone Belt: palaeoenvironmental and isotopic implications for the 2330–2060 Ma global isotope excursion of $^{13}\text{C}/^{12}\text{C}$. *Precamb. Res.* 133, 75–103.
- P.S., 1996. The internal structure of carbonate concretions in mudrocks: a critical evaluation of the conventional concentric model of concretion growth. *Sediment. Geol.* 103, 85–91.
- Ngombi-Pemba, L., 2014. *Géochimie et minéralogie des formations argileuses (2.2–2.0 Ga) du bassin de Franceville au Gabon: fluctuations de l'oxygène atmosphérique, chimie des océans et diagenèse au Paléoproterozoïque*. PhD Thesis, Poitiers University, 286 p.
- Ngombi-Pemba, L., El Albani, A., Meunier, A., Grauby, O., Gauthier-Lafaye, F., 2014. From detrital heritage to diagenetic transformations, the message of clay minerals contained within shales of the Palaeoproterozoic Francevillian basin (Gabon). *Precamb. Res.* 255, 63–76.
- Nothdurft, L.D., Webb, G.E., Kamber, B.S., 2004. Rare earth element geochemistry of Late Devonian reefal carbonates, canning basin, Western Australia: Confirmation of a seawater REE proxy in ancient limestones. *Geochim. Cosmochim. Acta* 68, 263–283.
- Oertel, G., Curtis, C.D., 1972. Clay ironstone concretion preserving fabrics due to progressive compaction. *Geol. Soc. Amer. Bull.* 83, 2597–2606.
- Ossa Ossa, F., El Albani, A., Hofmann, A., Bekker, A., Gauthier-Lafaye, F., Pambo, F., Meunier, A., Fontaine, C., Boulvais, P., Pierson-Wickmann, A.-C., Cavalazzi, B., Macchiarelli, R., 2013. Exceptional preservation of expandable clay minerals in the ca. 2.1 Ga black shales of the Francevillian basin, Gabon and its implication for atmospheric oxygen accumulation. *Chem. Geol.* 362, 181–192.
- Pisciotta, K.A., Mahoney, J.J., 1981. Isotopic survey of diagenetic carbonates, 63, Deep Sea Drilling Project (D.S.D.P.), pp. 595–609.
- Préat, A., Bouton, P., Thiéblemont, D., Prian, J.-P., Ndonze, S.S., Delpomdor, F., 2011. Paleoproterozoic high $\delta^{13}\text{C}$ dolomites from the Lastoville and Franceville basins (SE Gabon): Stratigraphic and synsedimentary subsidence implications. *Precamb. Res.* 189, 212–228.
- Pruysers, P.A., De Lange, G.J., Middelburg, J.J., 1991. Geochemistry of eastern Mediterranean sediments: primary sediments composition and diagenetic alteration. *Mar. Geol.* 100, 137–154.
- Raiswell, R., 1971. The growth of Cambrian and Liassic concretions. *Sedimentology* 17, 147–171.
- Raiswell, R., 1976. The microbiological formation of carbonate concretions in the Upper Lias of N.W., England. *Chem. Geol.* 18, 227–244.
- Raiswell, R., 1988. Chemical model for the origin of minor limestone-shale cycles by anaerobic methane oxidation. *Geology* 16, 641–644.
- Raiswell, R., Fisher, Q.J., 2000. Mudrock-hosted carbonate concretions: a review of growth mechanisms and their influence of chemical and isotopic composition. *J. Geol. Soc. Lond.* 157, 239–251.
- Ritger, S., Carson, B., Suess, E., 1987. Methane-derived authigenic carbonates formed by subduction-induced pore-water expulsion along the Oregon/Washington margin. *Geol. Soc. Amer. Bull.* 98, 147–156.
- Schrag, D.P., Higgins, J.A., Macdonald, F.A., Johnston, D.T., 2013. Authigenic carbonate and the history of the global carbon cycle. *Science* 339, 540–543.
- Taylor, S.R., McLennan, S.M., 1985. *The continental crust: its composition and evolution*. Blackwell, Oxford, 312 p.
- Thyne, G.D., Boles, J.R., 1989. Isotopic evidence for origin of the Moeraki septarian concretions, New Zealand. *J. Sedim. Petrol.* 59 (2), 272–279.
- Tribouillard, N., Algeo, T.J., Lyons, T., Riboulleau, A., 2006. Trace metals as paleoredox and paleoproductivity proxies: an update. *Chem. Geol.* 232, 12–32.
- Vasconcelos, C., McKenzie, J.A., Warthmann, R., Bernasconi, S., 2005. Calibration of the $\delta^{18}\text{O}$ paleo-thermometer with dolomite formed in microbial cultures and natural environments. *Geology* 33, 317–320.
- Veizer, J., 1989. Strontium isotopes in seawater through time. *Ann. Rev. Earth Planet. Sci.* 17, 141–167.
- Veizer, J., Hoefs, J., 1976. The nature of $^{18}\text{O}/^{16}\text{O}$ and $^{13}\text{C}/^{12}\text{C}$ secular trends in sedimentary carbonate rocks. *Geochim. Cosmochim. Acta* 40, 1387–1395.
- Velde, B. (Ed.), 1995. *Origin and Mineralogy of Clays*. Clays and the Environment. Springer-Verlag, Berlin, Heidelberg, New York, Barcelona, Budapest, Hong Kong, London, Milan, Paris, Tokyo, 334 p.
- Weber, F., 1969. Une série précambrienne du Gabon : le Francevillien. *Sédimentologie, géochimie, relations avec les gîtes minéraux associés*. Mém. Serv. Carte Géol. Alsace-Lorraine, Strasbourg, 328 p.
- Zheng, Y.F., 1999. Oxygen isotope fractionation in carbonate and sulfate minerals. *Geochemical J.* 33, 109–126.